Supplementary Information

Supplementary Figure S1

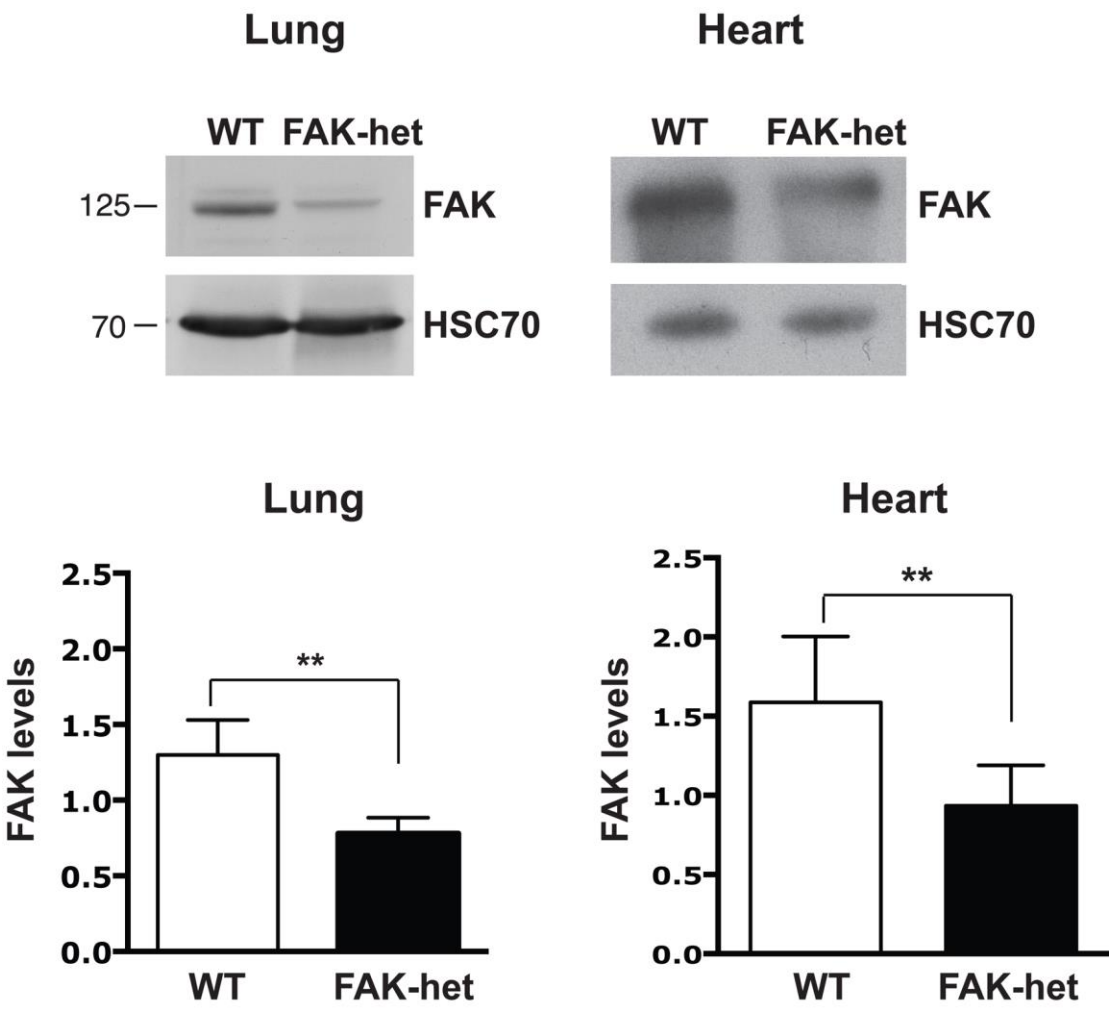

Supplementary Figure S1: Expression of FAK in unchallenged tissues.

Western blot analysis of lung and heart tissue extracts shows that FAK levels is reduced in FAK-heterozygous (FAK-het) compared with wild-type (WT) control mice. HSC-70 protein acted as a loading control. Bar chart presents the mean densitometry readings + s.e.m, n=4 mice per genotype, Student's t-test ***P<0.01*.

Supplementary Figure S2

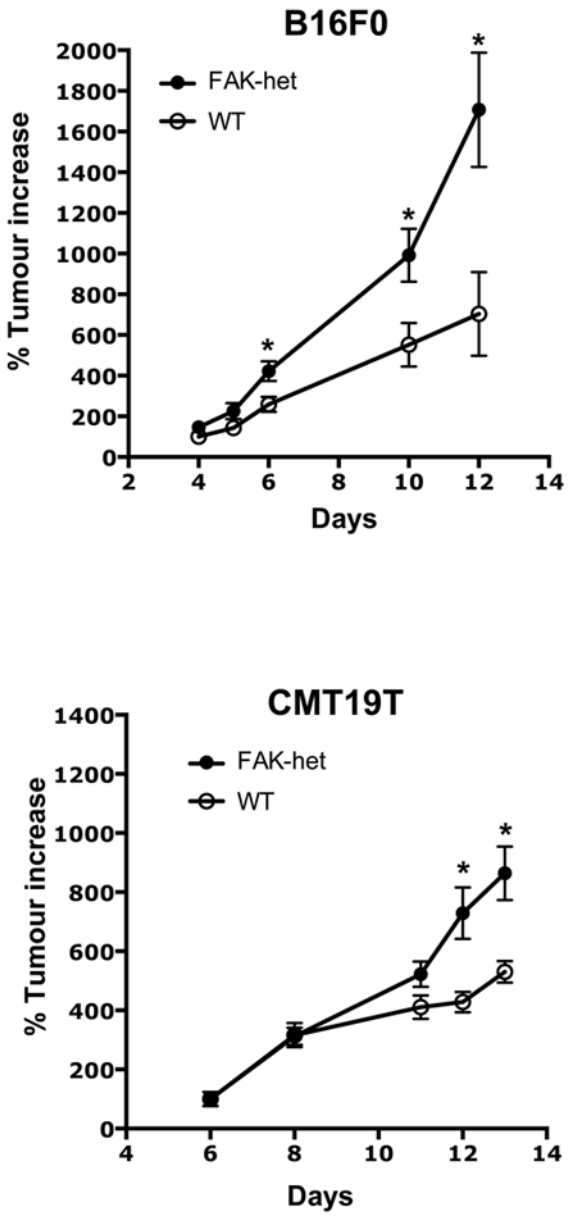

Supplementary Figure S2: FAK-heterozygous mice display enhanced tumour growth over time. B16F0 and CMT19T tumour cells were injected subcutaneously in FAK-heterozygous (FAK-het) and wild-type (WT) mice and their tumour size was measured over the course of 12-13 days. Graphs represent the % mean tumour volume increase ± s.e.m. n=9 WT and n=10 FAK-het mice for each tumour type, Mann-Whitney U rank sum test, **P<0.05*

Supplementary Figure S3

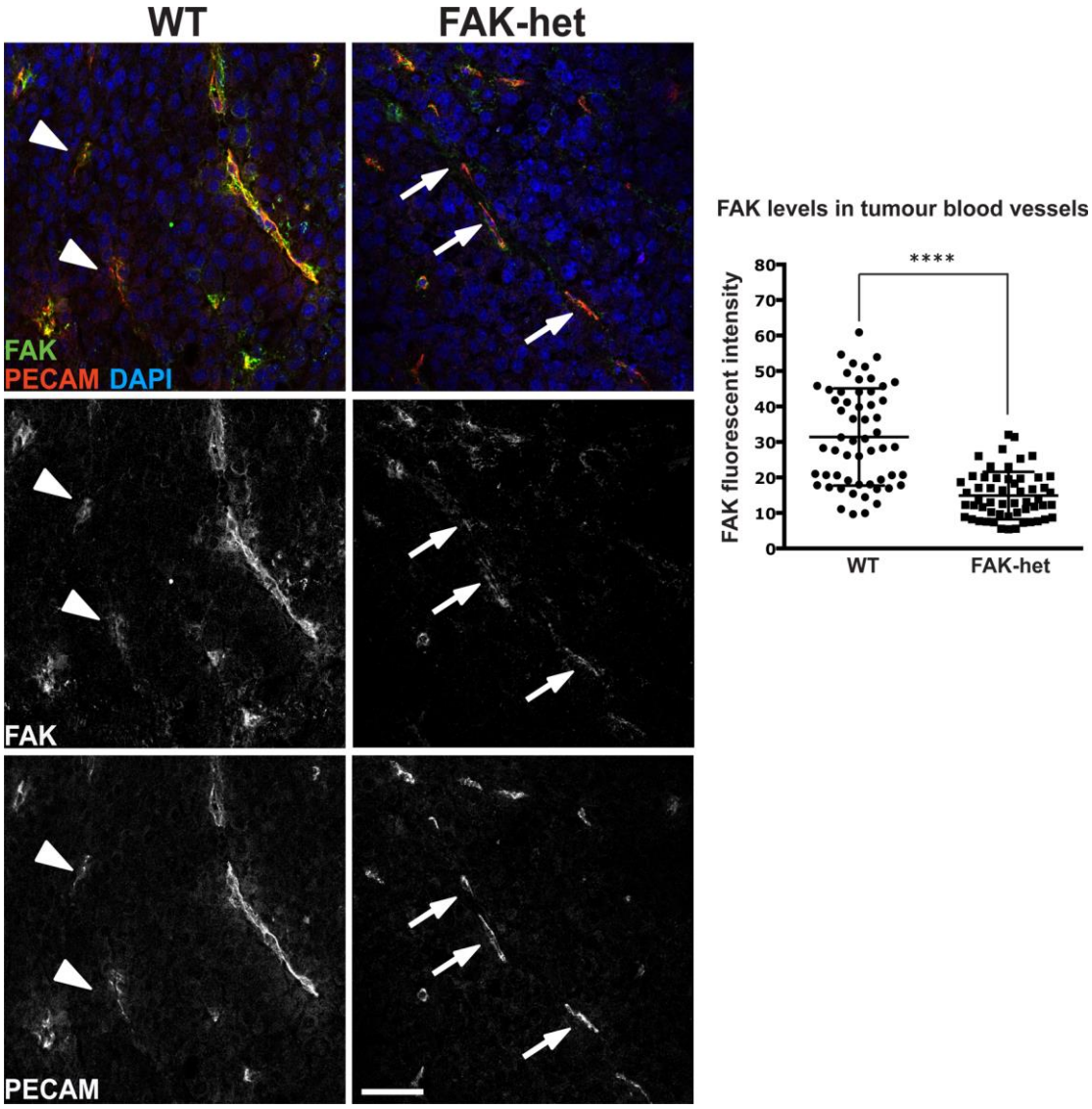

Supplementary Figure S3: FAK levels are reduced in tumour endothelium of FAK-heterozygous mice. Double immunofluorescence staining for FAK (green) and PECAM (red) of B16F0 tumour sections from FAK-heterozygous (FAK-het) and wild-type (WT) mice shows reduced blood vessel FAK levels by half in FAK-het compared with WT mice (*arrows*) and reveals a subpopulation of tumour blood vessels in WT mice that have similarly reduced FAK expression (*arrowheads*). DAPI (blue) was used as nuclei counterstain. Scatter plot chart shows the mean fluorescent intensity of FAK levels per blood vessel and the average value ± s.e.m of each

genotype. n=56 blood vessels from 10 tumours per each genotype, Student's t-test, ****$P<0.0001$. Scale bar 50μm.

Supplementary Figure S4

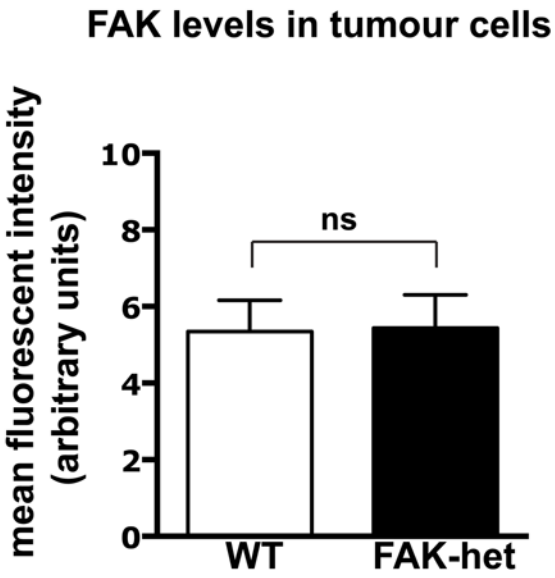

Supplementary Figure S4: FAK expression is not different in tumour cells grown in FAK-heterozygous and wild-type mice. Immunofluorescence analysis of FAK expression in B16F0 tumour cells grown in FAK-heterozygous (FAK-het) or wild-type (WT) mice shows no difference between genotypes. Bar chart represents mean fluorescent intensities of FAK in tumour compartment + s.e.m. n=9 WT and n=10 FAK-het tumours, Student's t-test, ns, not statistically significant different.

Supplementary Figure S5

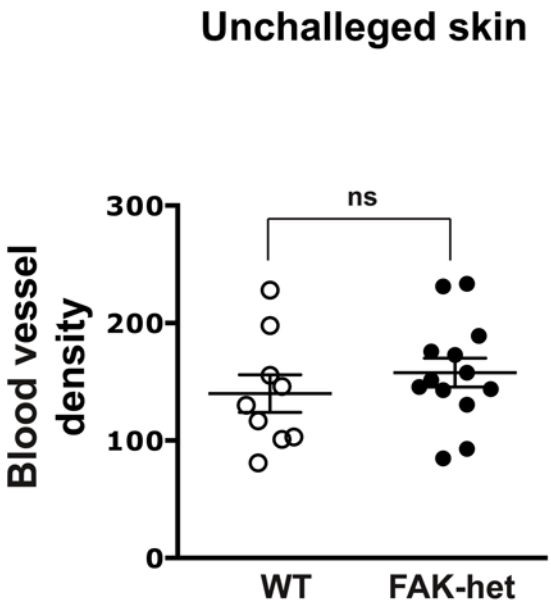

Supplementary Figure S5: FAK-heterozygosity does not affect blood vessel density in unchallenged skin. Blood vessel density in skin from FAK-heterozygous (FAK-het) and wild-type (WT) littermates was calculated as the number of blood vessels/mm^2 of transverse skin section. Scatter plot chart shows values of each skin section and the mean ± s.e.m. for each genotype. n= 9 WT and n=14 FAK-het mice, Student's t-test, ns, no statistically significant difference.

Supplementary Figure S6

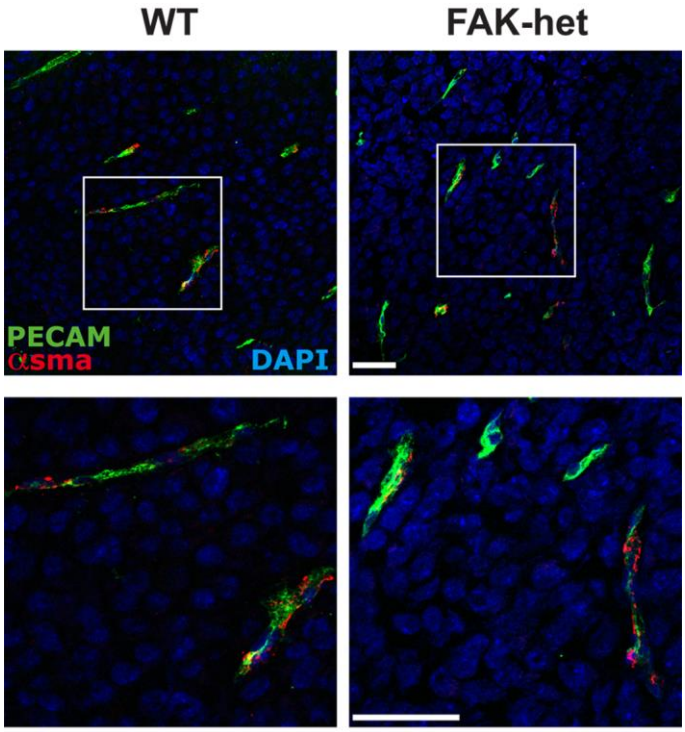

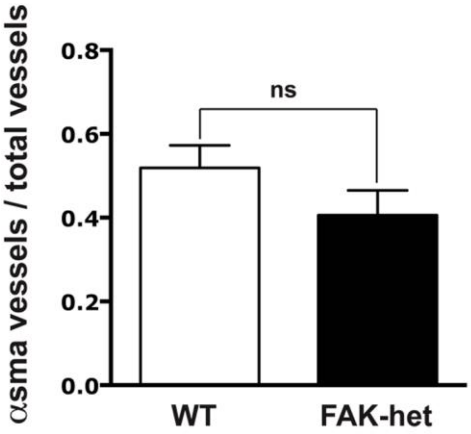

Supplementary Figure S6: FAK-heterozygosity does not affect the association of α-smooth muscle actin-positive pericytes with blood vessels. Double immunofluorescence staining of α-smooth muscle actin (α-sma, red) and PECAM (green) in B16F0 tumour blood vessels shows no significant difference in the proportion of blood vessels associated with α-sma-positive pericytes. DAPI (blue) was used as nuclei counterstain. Lower panels display magnification of the boxed areas. Bar charts represent the ratio of mean number of α-sma-positive vessels : total

number blood vessels + s.e.m. n=7 tumours per genotype, Student's t-test, ns, no statistically significant difference. Scale bar, 50μm

Supplementary Figure S7

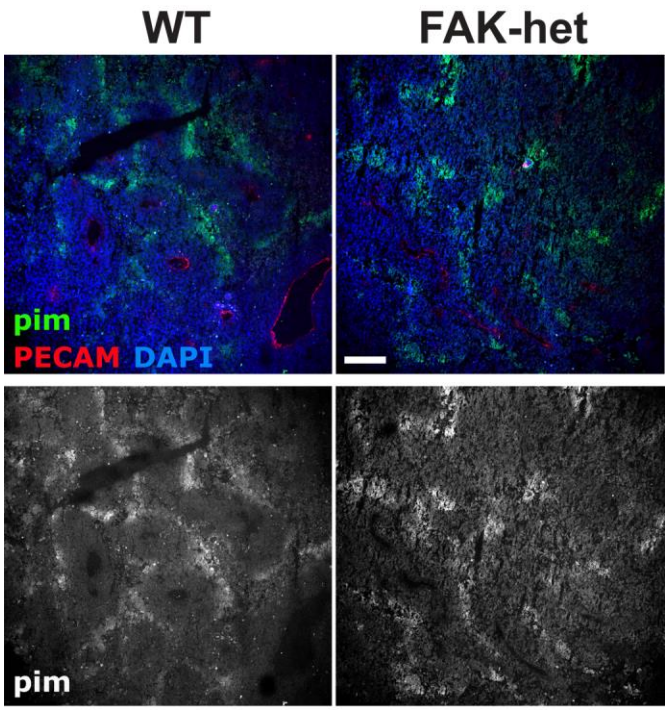

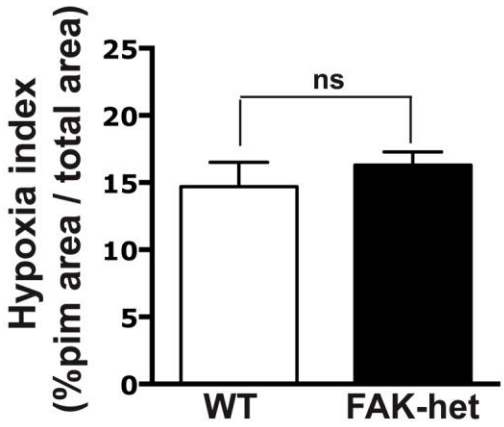

Supplementary Figure S7: Tumour hypoxia is not affected by stromal-FAK heterozygosity. Tumour hypoxia was detected by immunostaining of B16F0 tumour sections from FAK-heterozygous (FAK-het) and wild-type (WT) mice for pimonidazole adducts (green, white). PECAM (red) was used to detect blood vessels and DAPI (blue) was used as nuclei counterstain. Bar charts represent the hypoxic index of the tumour expressed as % mean area of pimonidazole stain / total area of tumour section + s.e.m. n=5 tumours per genotype, Student's t-test, ns, no statistically significant difference. Scale bar, 200μm

Supplementary Figure S8

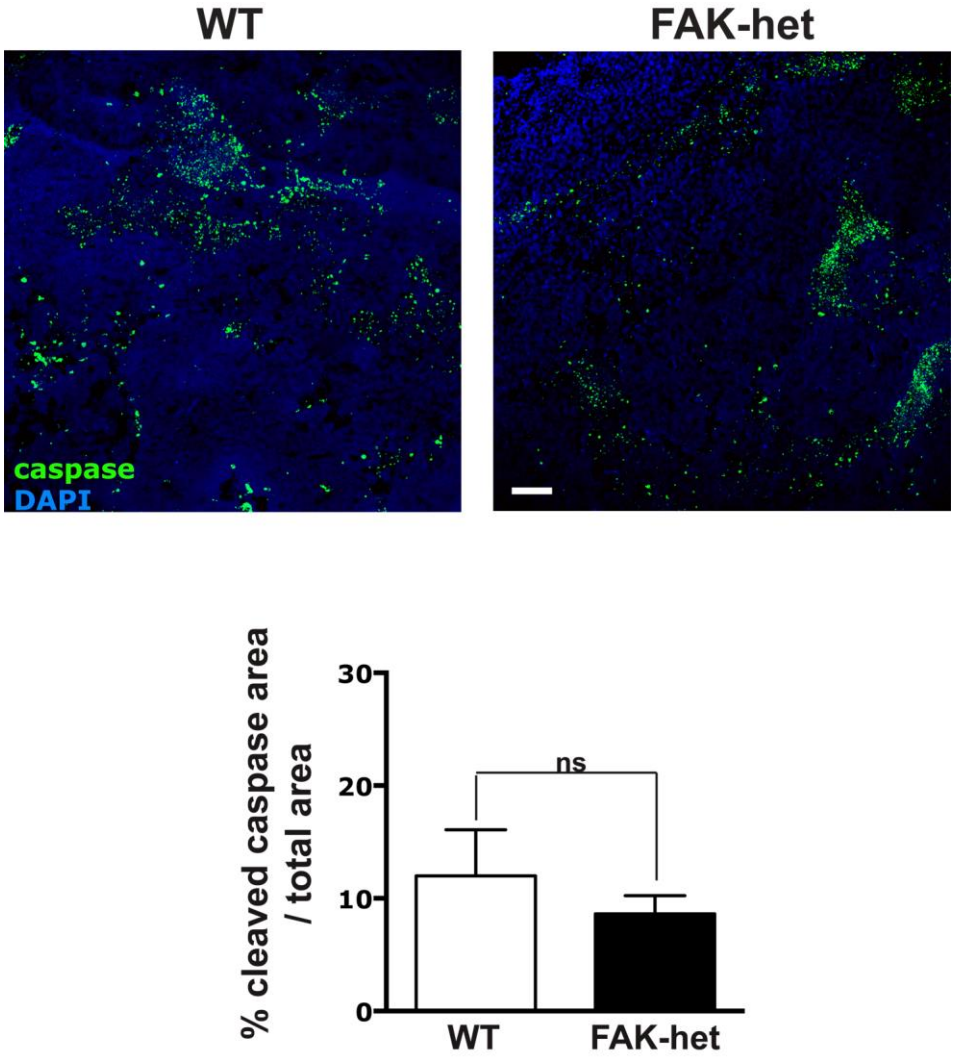

Supplementary Figure S8: Tumour apoptosis is not significantly altered in FAK-heterozygous mice. Tumour apoptosis was assessed by immunostaining for cleaved caspase 3 (green). DAPI (blue) was used as nuclei counterstain. Bar charts represent the apoptotic index of the tumour expressed as the % mean area of cleaved caspase stain / total area of tumour section + s.e.m. n=7 WT and n=10 FAK-het, Student's t-test, ns, no statistically significant difference. Scale bar, 200μm

Supplementary Figure S9

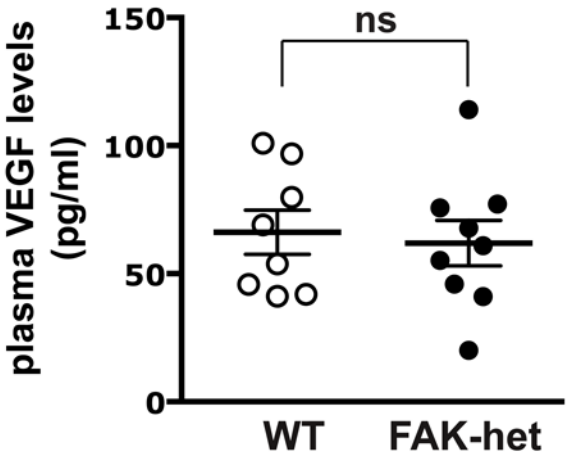

Supplementary Figure S9: VEGF production is unchanged in FAK-heterozygous mice. VEGF protein levels were assessed in blood plasma from FAK-heterozygous (FAK-het) and wild-type (WT) mice, using ELISA. Scatter plot chart represents the plasma VEGF protein of each sample and the mean ± s.e.m. for each genotype. n=8 WT and n=9 FAK-het mice, Student's t-test, ns, no statistically significant difference.

Supplementary Figure S10

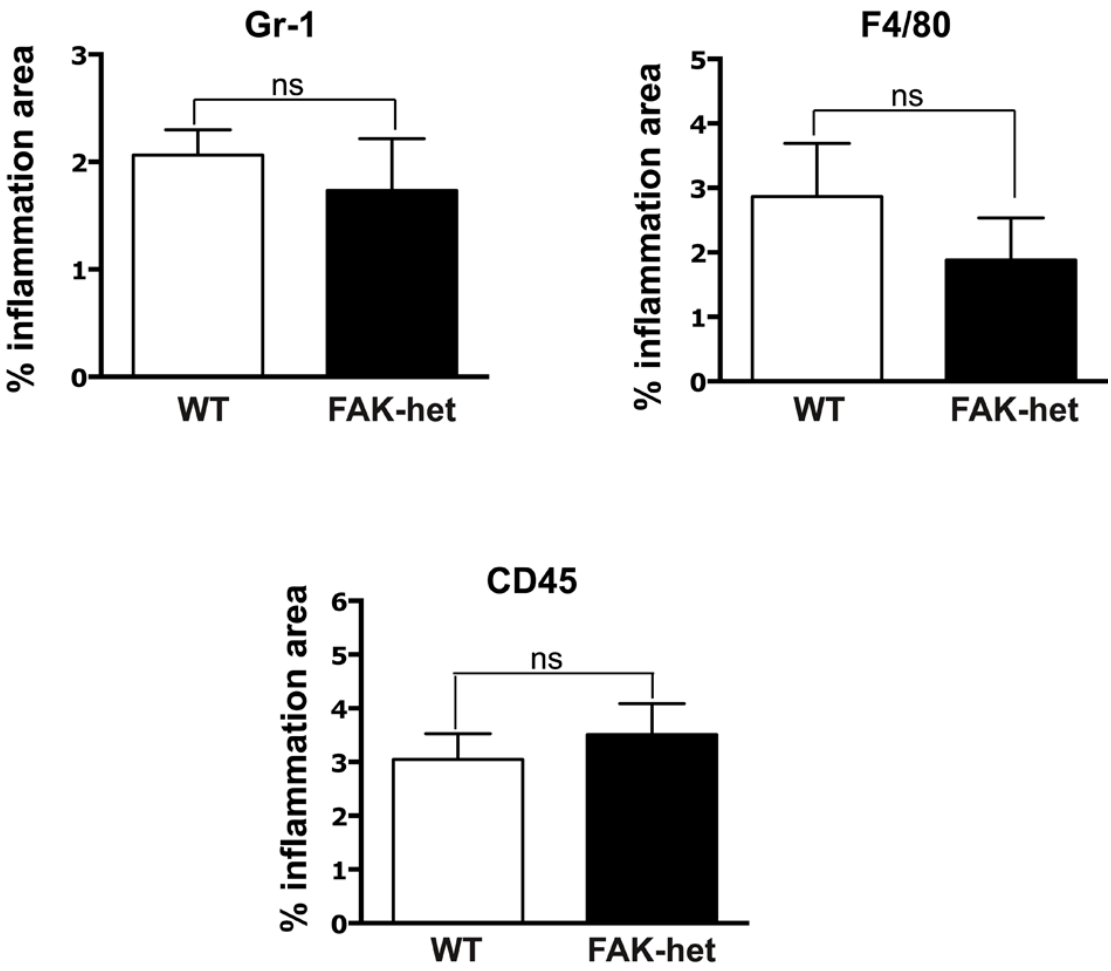

Supplementary Figure S10: Macrophage infiltration is not altered in FAK heterozygous mice. Sections of tumours from FAK-heterozygous (FAK-het) and wild-type (WT) mice were immunostained for Gr-1- and F4/80- positive macrophages and CD45-positive leukocytes. The area of inflammation was determined as the area of macrophage or leukocyte staining over the total area of tumour section. Bar charts represents % mean of inflammation area + s.e.m. n= 5 tumours per genotype for macrophage counts, n=6 WT and n=7 FAK-het for leukocyte counts, Student's t-test, ns, not statistically significant different.

Supplementary Figure S11

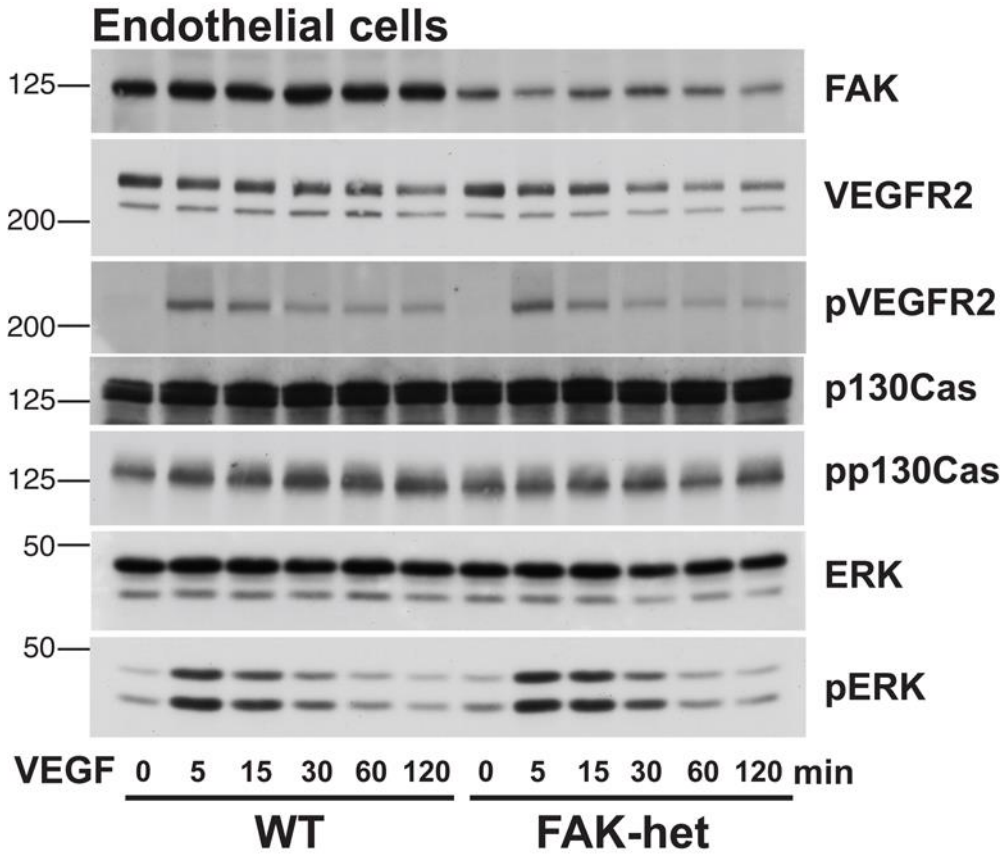

Supplementary Figure S11: FAK-heterozygosity does not affect VEGF-stimulated signalling in endothelial cells. Wild-type (WT) and FAK-heterozygous (FAK-het) ECs were stimulated with VEGF (30ng/ml for 0, 5, 15, 30, 60 and 120 minutes) and lysates used for assessing levels of FAK, VEGF-receptor 2 (VEGFR2), phosphorylated VEGFR2 (pVEGFR2), p130Cas, phosphorylated p130Cas (pp130Cas), total Erk1/2 and phosphorylated Erk1/2 (pErk1/2). Although FAK levels were clearly lower in FAK-het cells, no consistent changes in the expression or phosphorylation of other molecules were observed. Blots are representative of at least three independent experiments.

Supplementary Figure S12

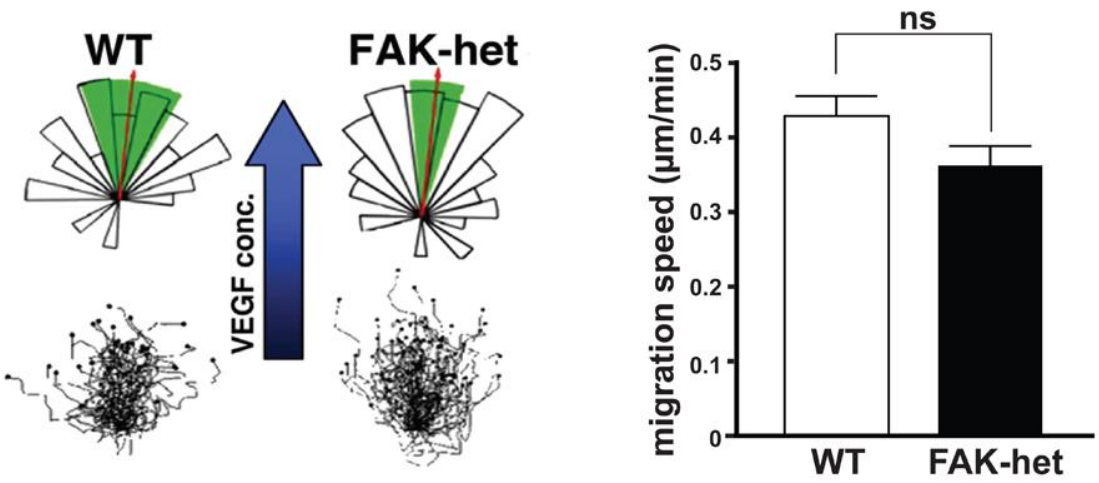

Supplementary Figure S12: FAK-heterozygous endothelial cells show no change in VEGF-stimulated migration. VEGF-stimulated migration was assessed in Dunn chambers for wild-type and FAK-heterozygous cells. Individual cells were tracked to determine statistically significant directional movement (green pie). The trend for directional movement in the whole population is indicated (red arrow). Bar chart presents the mean VEGF-stimulated cell migration speed + s.e.m. n=51 WT and n=72 FAK-het cells, Student's t-test, ns, not statistically significant different.

Supplementary Figure S13

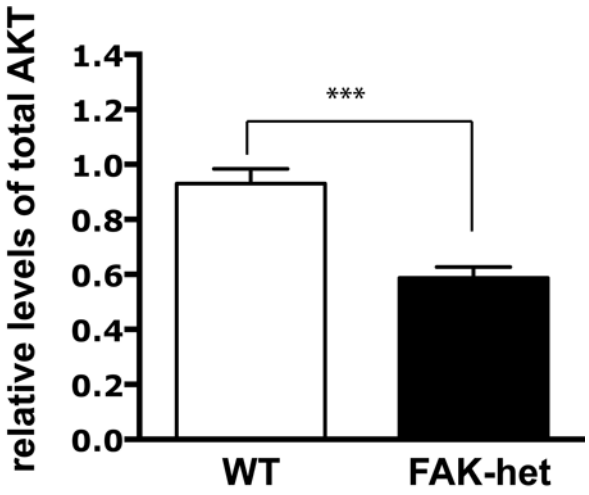

Supplementary Figure S13: Total Akt levels are decreased in FAK heterozygous endothelial cells. Quantification of western blot analysis of total Akt levels in FAK heterozygous (FAK-het) and wild-type (WT) endothelial cells. Bar chart represents mean densitometric readings normalised to WT +s.e.m. n=3 independent experiments, Student's t-test ***P<0.001*.

Supplementary Figure S14

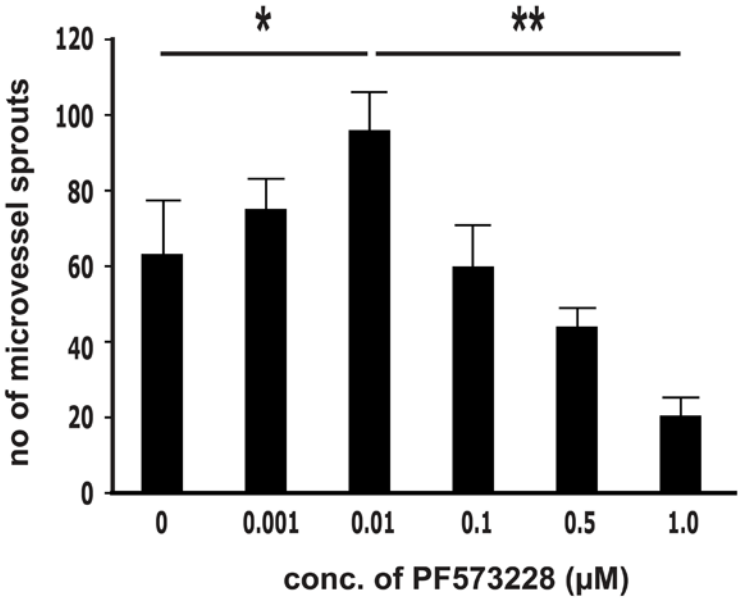

Supplementary Figure S14: Low doses of FAK inhibitor can enhance angiogenesis *ex vivo*. Serum-stimulated microvessel sprouting of WT aortic rings after treatement with the indicated doses of the FAK-inhibitor PF-573228. 1μM PF-573228 inhibited microvessel sprouting. In contrast 0.01μM PF-573228 enhanced significantly microvessel sprouting. Bar chart represents the mean number of serum-stimulated (2.5%) microvessel sprouts per aortic ring + s.e.m. n=30 aortic rings per treatment, Student's t-test **P<0.05, **P<0.01*.

Supplementary Figure S15

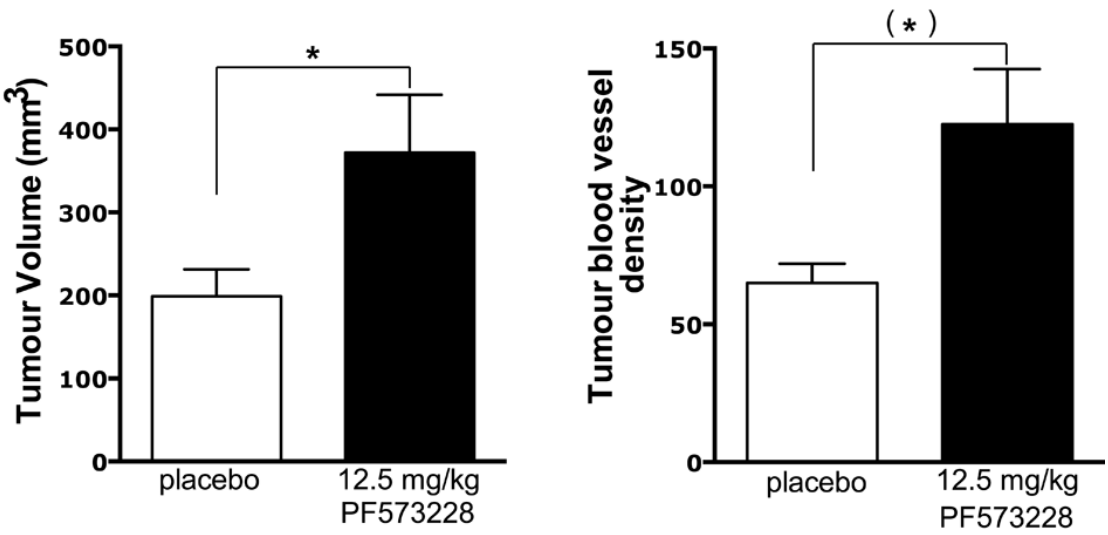

Supplementary Figure S15: Low doses of FAK inhibitor can enhance tumour growth and angiogenesis. Wild type mice were injected with B16F0 tumour cells and treated with a suboptimal dose of the FAK inhibitor PF-573228 (12.5mg/Kg). Treatment with 12.5mg/Kg PF-573228 enhances *in vivo* tumour growth and angiogenesis of B16F0 tumours when compared with placebo treated controls. Left bar chart represents B16F0 tumour size at day 11 after tumour cell inoculation in WT mice treated with 12.5mg/Kg PF-573228 or placebo. Right bar chart represent mean tumour blood vessel densities for the same mice. All values are given mean + s.e.m. n= 9 placebo-treated and n=8 PF-573228 –treated mice, Student's t-test *P<0.05, $^{(*)}$ P=0.05.

Supplementary Methods

Immunofluorescence detection of FAK-levels in B16F0 tumour cells *in vivo*.

To analyse the FAK protein levels in blood vessels and tumour cells *in vivo*, snap-frozen tumour sections were fixed for 5 minutes in acetone : ethanol 3:1, washed 3x with PBS and double stained for mouse anti-FAK and rat anti-PECAM antibodies (1:100, BD Biosciences cat. no. 610087 and 550274) overnight, followed by 1 hour incubation with anti-mouse Alexa-Fluor®-488 and anti-rat Alexa-Fluor®-555 conjugated secondary antibodies (1:400, Invitrogen A11029 and A21434) and mounted using Prolong® Gold anti-fade reagent (Invitrogen) with DAPI. Non-saturated images were acquired using confocal laser microscopy (Leica SP5) with identical laser settings (47% for 405, 50% for 488, 48% for 561) gain (778 for 405, 727 for 488, 741 for 561) and offset (-2 for all laser lines) resulting in unsaturated pixel intensities for all tumour sections of both WT and FAK-heterozygous mice. Using the signal intensity of the PECAM staining, region of interest (ROI) were manually drawn delineating the area covered by ECs of each blood vessel. To quantify FAK expression in tumour cells, ROI comprised only by tumour cells and not containing any blood vessels were randomly selected. The signal intensity of FAK staining in these ROI was calculated using the Leica SP5 software.

Examining inflammation in tumours

Briefly, cryostat sections from tumours were treated with 0.5% NP-40 and blocked with 2% normal goat serum, 1% BSA and 0.1% Triton-X100. Sections were incubated with the primary anti-F4/80 (1:50, AbD Serotec MCA497), anti-Gr-1 (1:50, BD Biosciences, cat. no RM3000) or anti-CD45 (1:200, Biolegend, cat. no 103102) antibody overnight at 4^{o}C, followed by an Alexa-Fluor®-488 -conjugated secondary antibody (Invitrogen) for 1 hour at room temperature. Samples were mounted with

Gelvatol (Millipore) supplemented with DABCO anti-fading agent (Sigma). Cell nuclei were detected by DAPI. Fluorescence images were captured using a CCD camera Hamamatsu C4742-95 and a Zeiss Axioplan microscope. Areas with infiltrated macrophages were outlined and measured, using the AxioVision Imaging Software (Carl Zeiss). The percentage of the inflammation area was calculated as the ratio of the tumour section area that was Gr1-positive, F4/80-positive or CD45-positive over the total area of tumour section.

Hypoxia detection in tumours

Wild-type and FAK-heterozygous mice with subcutaneous B16F0 tumours were injected i.p. with 60mg/kg of pimonidazole 1 hour before tumour dissection. Hydroxyprobe-1 Plus Kit (Natural Pharmacia International) was used following the manufacturer instructions. Fluorescence images were captured using a CCD camera Hamamatsu C4742-95 and a Zeiss Axioplan microscope. The area positive for staining were outlined and measured using the AxioVision Imaging Software (Carl Zeiss). The hypoxic index of the tumour was calculated as the area of pimonidazole staining / area of tumour section.

Detection of tumour apoptosis

Snap-frozen tumour sections were fixed in acetone for 10 minutes and blocked with PBS containing 1%BSA, 0.2% Triton-X for 30 minutes at room temperature. Sections were incubated with cleaved caspase-3 antibody (1:100, Cell Signalling cat.no 9579) overnight at 4ºC. Sections were washed three times in PBS- 0.01% Tween-20, incubated with anti-rabbit Alexa-Fluor®-488 conjugated secondary antibodies and mounted using Prolong® Gold anti-fade reagent (Invitrogen) with

DAPI. Fluorescence images were captured using a CCD camera Hamamatsu C4742-95 and a Zeiss Axioplan microscope. The area containing caspase-positive cells was outlined and measured using the AxioVision Imaging Software (Carl Zeiss). Necrotic tumours with higher than 60% of caspase-positive area : total area of section were excluded. The apoptotic index of the tumour was calculated as the area of cleaved caspase staining / area of tumour section.

Western blotting

Wild-type and FAK-heterozygous endothelial cells were serum starved for 4 hours and then stimulated with 30ng/ml of VEGF for the indicated times before lysing. Cells were then washed 3 times in cold PBS and lysed in sample buffer (without bromophenol blue). To prepare protein extracts from lung and heart, tissues were palpitated in dry ice and lysed in sample buffer (without bromophenol blue). Lysed samples were sonicated briefly, and total protein was quantified using *DC* Protein Assay (Bio-Rad). Beta-mercaptoethanol was added to the samples and these were routinely separated on 10% sodium dodecyl sulphate–polyacrylamide gel electrophoresis gels. Briefly, nitrocellulose membranes (Millipore) were blocked in blocking buffer (either 5% BSA or milk in Tris-buffered saline 0.1% Tween-20) for 1 hour. Membranes were then incubated with 1:1000 diluted primary antibodies in blocking buffer overnight at 4°C, washed three times, before incubation with HRP-conjugated secondary antibodies in blocking buffer for 1 hour at room temperature. Antibodies used for Western blotting were purchased from the following companies: p130Cas antibody from Millipore (cat. no 06-500), rabbit anti-phospho-p130Cas, anti-VEGFR2 and the anti-phospho-VEGFR2 antibodies were all from Cell Signaling Technologies (cat. no 4014, 2479, 2478, respectively).

Detection of VEGF levels *in vivo*.

Blood samples were obtained from wild-type and FAK-heterozygous mice by exsanguination. The plasma fraction was isolated by centrifugation at 3000rpm for 10min. The VEGF protein content was assessed using a mouse-specific VEGF ELISA kit (RnD Systems) according to the manufacturer instructions. The absorbance of the samples at 450 was measured using an Anthos 2001 microplate reader.

***Ex vivo* aortic ring assay with FAK inhibitor**

Thoracic aortas were isolated and prepared for culture as described previously[23]. Briefly, 1mm thick rings were serum starved for 18 hours at 37ºC before being embedded in growth factor-reduced Matrigel™ (BD Biosciences) and cultured in medium supplemented with 2.5% foetal calf serum (FCS) with or without PF-573228 FAK inhibitor (Pfizer) at concentrations indicated. Rings were fed every 2 days with fresh medium containing 2.5% FCS and the indicated concentration of the inhibitor. Sprouting microvessels were counted after 6 days.

Tumour growth and blood vessel density with FAK inhibitor

To analyse the effect of FAK inhibition in tumour growth, C57Bl6 mice were injected subcutaneously with 1x 10^6 B16F0 cells. When tumours became palpable (day 7 post-inoculation) mice were i.p injected twice everyday with 12.5mg/Kg PF573228 inhibitor (Pfiser Inc) dissolved in 5% DMSO or equal volume of 5% DMSO, as placebo. Tumour dimensions were measured after dissection on day 11 after tumour

cell injection and calculated as length x width^2 x 0.52. Size matched tumours were analysed for blood vessel density as described in the main text.